International Journal of Refrigeration
35 (2012) 1410 - 1417

# Effect of lubricating oil on the flow and heat transfer characteristics of supercritical carbon dioxide

Chaobin DANG*, Keitaro HOSHIKA, Eiji HIHARA

Department of Human and Engineered Environment, Graduate School of Frontier Sciences, The University of Tokyo, Kashiwa-Shi, Chiba, Japan
Tel./Fax: 81-47-136-4647, dangcb@k.u-tokyo.ac.jp
*Corresponding Author

## ABSTRACT

Effects of lubricating oil on heat transfer performance of supercritical $CO_2$ were studied by applying three lubricants: PAG, PVE, and ECP. Heat transfer coefficient measurements and flow-pattern visualization were conducted in a horizontal tube of 2 mm I.D. at $CO_2$ pressures from 8 to 10 MPa and mass fluxes from 800 to 1200 kg $m^{-2}s^{-1}$. The solubility of lubricants with $CO_2$ was found having remarkable influence on both the flow pattern and heat transfer coefficient. For PVE, which has the highest $CO_2$ solubility, oil droplets can only be observed occasionally and the oil film can hardly be identified at temperatures lower than $T_{pc}$, and the heat transfer coefficient does not greatly change with oil concentration. At higher temperatures, a decrease in the heat transfer coefficient with increasing oil concentration was observed for all three lubricants due to the formation of oil film. The experiments show that while ECP is inferior to PVE, it provides better heat transfer performance than PVG.

**Keywords:** $CO_2$, Lubricat, heat transfer, Polyalkylene glycol, Polyvinyl ether, ECP

## NOMENCLATURE

| | | | | |
|---|---|---|---|---|
| $A$ | surface area | ($m^2$) | **Subscripts** | |
| $\alpha$ | heat transfer coefficient | (W $m^{-2}K^{-1}$ ) | $CO_2$ | $CO_2$ |
| $G$ | mass flux | (kg $m^2s^{-1}$) | *in* | inlet |
| $P$ | pressure | (MPa) | *oil* | oil |
| $Q$ | heat exchange rate | (W) | *pc* | pseudocritical |
| $x$ | oil concentration | (wt%) | *out* | outlet |
| $T$ | temperature | (°C) | *w* | wall |
| $\Delta T$ | average temperature difference | (°C) | *water* | water |
| $\phi$ | deterioration factor | | | |

## 1. INTRODUCTION

Carbon dioxide, $CO_2$, is being reintroduced as an environmentally benign working fluid for refrigeration and air conditioning systems because of increasing concerns regarding the contribution of conventional refrigerants to ozone depletion and global warming. Owing to its low critical point, a transcritical cycle is proposed for $CO_2$ systems. A great deal of research has been carried out on transcritical heat pump cycles and heat transfer characteristics of $CO_2$ at both supercritical and subcritical pressure. Previous studies such as those by Tanaka *et al.* (1967), Fang *et al.* (2001), and Dang *et al.* (2004) showed that the heat transfer characteristics of $CO_2$ at

supercritical pressure differ from those of fluids with constant properties. $CO_2$ has a better heat transfer performance owing to its low viscosity and high specific heat, especially within the pseudocritical temperature region. However, because of the entrainment of lubricating oils, both the heat transfer performance of $CO_2$ and the system performance in an actual heat pump system may be markedly worse than the predicted value for pure $CO_2$. Therefore, it is essential to clarify the effects of lubricating oils on the heat transfer characteristics of $CO_2$.

Hwang *et al.* (2007) experimentally investigated the distribution of PAG (polyalkylene glycol) oil in a $CO_2$ transcritical system by measuring the amount of oil retained in the suction line, evaporator, and gas cooler at various refrigerant mass flow rates and oil concentrations. They reported that about 50% of the oil was retained within the heat exchangers and suction line; this resulted in a large pressure drop, a decrease in the heat transfer performance, and concern regarding the reliability of the system. Zingerli and Groll (2000) measured the heat transfer coefficient and pressure drop of a $CO_2$-POE (polyol ester) mixture at three oil concentrations—0%, 2%, and 5.0%—in a tube with a 2.85-mm I.D. Their results showed a 15% decrease in the heat transfer coefficient at an oil concentration of 2% and a 25% decrease at a concentration of 5%, within the near-pseudocritical temperature region. However, they also reported that the heat transfer was promoted at high temperatures. Gao and Honda (2002) investigated the heat transfer characteristics of supercritical $CO_2$ with PAG oil and reported a maximum decrease of 40% at an oil concentration of 1%. Dang *et al.* (2007, 2008) investigated the flow pattern and heat transfer characteristics of a $CO_2$-PAG oil mixture in horizontal tubes with I.D. ranging from 1 mm to 6 mm. A significant influence of the oil on the heat transfer was confirmed for a small-diameter tube at a large oil concentration. The decrease in the heat transfer was due to the formation of an oil-rich layer along the walls of the test tube. In addition, Yun *et al.* (2006) investigated the effects of oil on the heat transfer characteristics of supercritical $CO_2$ within a microchannel with a hydraulic diameter of 1.0 mm. They measured the cooling heat transfer coefficient and pressure drop of the oil-PAG mixture at oil concentrations of 0%–4% and pressures of 8.4 MPa and 10.4 MPa. The results showed that the average heat transfer coefficient decreased by 9.6% at an oil concentration of 2% and by 20.4% at a concentration of 4% as compared with that of pure $CO_2$.

Most of the above studies concentrated on the effect of PAG oil because it is the most widely used lubricant in $CO_2$ heat-pump water heaters. PAG oil shows excellent compatibility with $CO_2$, but the solubility of $CO_2$ in PAG oil is poor, leading to difficulties in oil return and deterioration of the heat transfer performance. Several new lubricating oils have been developed for $CO_2$ heat pumps (e.g., Sawada 2008, Kaneko et al. 2008), but their effects on the heat transfer performance are unclear. In this study, we investigated three lubricants for $CO_2$ systems—PAG, polyvinyl ether (PVE), and a newly proposed PAG-PVE copolymer (ECP)—to clarify the flow patterns of $CO_2$-oil mixtures and their influence on the heat transfer characteristics of supercritical $CO_2$.

## 2. COMPARISON OF LUBRICATING OILS

Lubricating oil is commonly used in compressors for lubrication, cooling, and sealing. PAG-type oil is commonly used for $CO_2$ heat pumps, although its viscosity changes with the compressor design of the manufacturer. Kaneko *et al.* (2006) compared PAG oil with POE oil and considered the following five aspects: -40 °C starting torque, oil return, shue/plate lubricity, bearing fatigue life, and stability. They reported that, with the exception of oil return, PAG oil is superior to POE oil in all these five aspects. With the widespread use of $CO_2$ heat-pump water heaters in Japan, the development of new lubricating oils is underway. Sawada (2008) reported a

new POE oil showing better lubricity and stability with $CO_2$ under supercritical conditions. Kaneko *et al.* (2008) developed ECP oil, which is a PAG-PVE-type copolymer oil. It has been reported that ECP oil retains not only the good stability and lubricity of PAG oil but also has better viscosity.

Three lubricating oils—PAG, PVE, and ECP—were tested in this research in order to verify the effects of oil on the flow pattern and heat transfer performance of supercritical $CO_2$. The ECP oil is a copolymer of PAG and PVE oils and has a solubility and viscosity between those of PAG and PVE. Table 1 shows the molecular structure, viscosity and thermal conductivity of the three lubricants. For both lubricants, the viscosity decreases dramatically with temperature whereas the thermal conductivity decreases slightly with temperature. PAG has the largest viscosity while PVE has the smallest value. The viscosity of ECP lies between those two values. In addition, there is no significant difference in thermal conductivity among the three oils as shown in Table 1. Figure 1 shows the two-phase separation temperature of these three oils with $CO_2$ under subcritical conditions. Among the three oils, PVE has the smallest separation region and PAG has the largest. Although the temperature for two-phase separation under supercritical conditions is yet to be determined, it is easy to deduce that PVE has the best miscibility with supercritical $CO_2$ whereas PAG has the worst. When the oil separates from supercritical $CO_2$, some $CO_2$ may dissolve in the oil, leading to a decrease in oil viscosity and surface tension. Both the thermophysical properties of $CO_2$ and its solubility in oil change with temperature inside the gas cooler, resulting in difficulties in predicting the flow pattern and heat transfer characteristics of the $CO_2$-oil mixture.

## 3. EXPERIMENTAL APPARATUS AND DATA REDUCTION

### 3.1 Experimental Loop

The experimental loop shown in Fig. 2 is composed of three parts: a main loop, a test loop, and an oil-adjustment loop. The main loop is a $CO_2$ heat-pump cycle that supplies supercritical $CO_2$ to the test section at the desired temperature and pressure. The test loop includes a heat-transfer test section, a visual section, and an oil-sampling section. The heat-transfer test section is a tube-in-tube-type heat exchanger with a length of 0.5 m, as shown in Fig. 3. Supercritical $CO_2$ flows through the inner section of the smooth horizontal tube having an inner diameter of 2 mm and is cooled by the water flowing inside the annular passage. The inner and outer tubes are made of smooth copper and acrylic resin, respectively. The external tube of the acrylic resin was covered with polystyrene insulation layer having a thickness of 25 mm to minimize heat loss to the environment. Pt100 sensors were used to measure the temperatures of $CO_2$ and water at the inlet and outlet of the test section. The wall temperature was measured at ten locations using type-T thermocouples placed evenly along the tube. The inner wall temperatures at the ten locations were calculated from the corresponding outer wall temperatures by solving one-dimensional heat conduction equations. The thermocouples and Pt100 sensors were calibrated to an accuracy of ±0.1 ºC and ±0.03 ºC, respectively. The $CO_2$ pressures at the inlet and outlet of the test section were measured using a pressure transducer with a measurement uncertainty of ±0.001 MPa. The mass flow rate of the refrigerant was measured using a Coriolis-type mass flow meter with an accuracy of 0.1% F.S. The accuracy of the water-side mass-flow rate was 0.5% F.S.

The visualization section was located behind the test section. The visualization images were

recorded through a sight glass using a high-speed CCD camera with a maximum speed of 70,000 fps. The assembled sight glass, shown in Fig. 4, is made of sapphire and can withstand a pressure of up to 20 MPa. The inner diameter of the sapphire tube is 2 mm with a glass thickness of 14 mm. Because the refractive index of the sapphire glass is 1.76, which is much higher than the refractive index of air, the sight glass was placed in a water box to reduce the refraction of the incoming light while passing through the glass.

The concentration of oil was controlled by adjusting the amount flowing into the test section using an oil flow meter and a needle valve. The oil-sampling section was placed behind the test section, and the temperature of $CO_2$ was maintained at 25 ˚C using a sub-cooler. Inside the oil-sampling section, the refrigerant-oil mixture was sampled, and the concentration of the lubricating oil in the refrigerant was weighed by releasing the refrigerant carefully using a needle valve. It should be noted that the measured oil concentration is actually the oil retention ratio, not the oil circulation ratio. Although the oil circulation ratio is simultaneously recorded using an oil flow meter, the amount of oil retained is used to define the oil concentration, to maintain consistency with our previous research (e.g., Dang *et al.* (2007, 2008)).

### 3.2 Experimental Conditions and Data Reduction

The experimental parameters considered in this study were mass flux, pressure, oil type, and oil concentration, as shown in Table 2. Under each experimental condition, the $CO_2$ inlet temperature was varied from 30 ºC to 70 ºC. The concentration of the PAG, PVE, and ECP lubricating oils were varied from 0.5–5.0 wt%.

The heat transfer coefficient was calculated from the heat flux and average temperature difference between the refrigerant and wall:

$$\alpha = \frac{Q_{\text{water}}}{A \cdot \Delta T_{\text{LMTD}_{\text{Water}}}}, \tag{1}$$

where $Q_{water}$ is calculated from the heat exchange rate of the waterside, as shown in equation (2).

$$Q_{water} = M_{water} \cdot C_{pwater} \left( T_{water,out} - T_{water,in} \right) \tag{2}$$

The mean temperature difference $\Delta T$ is defined as follows:

$$\Delta T_{\text{LMTD}_{\text{w}}} = \frac{\left( T_{\text{CO}_2\text{in}} - T_{\text{w,in}} \right) - \left( T_{\text{CO}_2\text{out}} - T_{\text{w,out}} \right)}{\ln\left( \frac{T_{\text{CO}_2\text{in}} - T_{\text{w,in}}}{T_{\text{CO}_2\text{out}} - T_{\text{w,out}}} \right)} \tag{3}$$

To evaluate the deterioration in the heat transfer coefficient by the entrainment of the different oils, a deterioration factor, $\phi$, is defined as follows:

$$\phi = \frac{\alpha_{CO_2} - \alpha_{CO_2-oil}}{\alpha_{CO_2}} \tag{4}$$

where $\alpha_{CO_2}$ denotes the heat transfer coefficient of pure $CO_2$ and $\alpha_{CO_2-oil}$ denotes the heat transfer coefficient of the $CO_2$-oil mixture under the same experimental conditions. According to the above definition, a large $\phi$ value corresponds to a large deterioration in the heat transfer coefficient of the fluid as compared to that of pure $CO_2$.

## 4. EXPERIMENTAL RESULTS AND DISCUSSION

### 4.1 Flow Visualization

Because of the different solubility of $CO_2$ in the three oils tested, the flow patterns of the $CO_2$-oil mixtures were different even at the same oil concentration, resulting in differences in the heat transfer coefficient. Fig. 5 shows a comparison of the flow pattern of $CO_2$ with PVE, ECP, and PAG. Note that the flow pattern of the $CO_2$-PAG mixture is obtained from our previous research (Dang *et al.* 2008), and the bright strip in the middle is due to the refraction of the incoming light because the refractive index of sapphire glass is much higher than that of air. The comparison was conducted at three temperatures—30˚C, 35˚C, and 40˚C—to study the change in the flow pattern at temperatures higher or lower than the pseudocritical temperature, i.e., 34.5 ˚C at a pressure of 8 MPa. Fig. 5(a) shows the flow pattern of the $CO_2$-PVE mixture. When the bulk temperature is lower than the pseudocritical temperature, PVE becomes miscible with $CO_2$, i.e., the oil film can hardly be identified, and oil droplets are only occasionally observed. In contrast, Fig. 5(b) shows that a thin oil film can be observed, together with a number of oil droplets scattered inside the bulk $CO_2$, indicating that the ECP oil is partially miscible with $CO_2$. From Fig. 5(c), it can be seen that most of the PAG oil adheres to the inner surface of the tube and forms a thick oil film in comparison to that of Fig. 5(b) because of the poor miscibility of PAG oil with $CO_2$. The tiny strip of oil-rich layer is visible and moves at a slow velocity.

When the inlet temperature of $CO_2$ approaches the pseudocritical temperature, it can be seen from Figs. 5(a) and 5(b) that the number of droplets of both PVE and ECP increases because of the decrease in the solubility of $CO_2$ in the oil. For PVE, the oil film is not easy to identify, whereas for ECP, the number of oil droplets increases with temperature, and the oil film thickens and can be identified as a narrow strip flowing along the inner surface. For PAG, the oil film is clearly observed at 35 ºC as shown in Fig. 5(c), but the number of oil droplets decreases, implying that part of the separated oil flowing with the bulk $CO_2$ adheres to the inner wall, forming a thicker layer. The main reason for the change in the flow pattern is the drastic changes in the properties of $CO_2$ within the pseudocritical region, including changes in the $CO_2$ density, solubility of $CO_2$ in the oil, and viscosity of the oil layer.

When the temperature increases above the pseudocritical temperature, the oil film thickens for all three lubricants because of the increase in the density ratio of $CO_2$ to oil. In addition, the reduction in the solubility of $CO_2$ leads to an increase in the viscosity and surface tension, both of which are positive effects for the stabilization of the oil layer. For PVE, both the number of oil droplets flowing with $CO_2$ and the thickness of the oil layer increase with temperature, implying a decrease in the miscibility of PVE oil with $CO_2$. In contrast, the number of ECP oil droplets decreases, showing that more oil droplets attach to the wall surface. For PAG, only an oil film with a wavy surface and a few oil droplets can be observed. The differences in the flow patterns are mainly a result of the different miscibility between the oils and $CO_2$.

The flow visualization of $CO_2$ within the entrained oil and the classification of flow patterns by Dang *et al.* (2008) suggest that the dominating flow pattern of $CO_2$-PVE and $CO_2$-ECP is an annular-dispersed flow from a bulk temperature of 30 ºC to 40 ºC. For PAG, the flow pattern changes from an annular-dispersed flow to a wavy flow as the bulk temperature increases.

### 4.2 Comparison of heat transfer coefficient

The heat transfer coefficients of $CO_2$ with the different oils are compared with that of pure $CO_2$ in Figs. 6–8 using mass flux, pressure, inlet temperature, and oil concentration as parameters. The predicted values of pure $CO_2$ (Dang and Hihara, 2004) are indicated by solid lines, and the heat transfer coefficients measured at different oil concentrations are plotted using a horizontal error bar representing the temperature change inside the test section. The oil

concentration is determined by a sampling method. The value in parentheses indicates the oil concentration measured using a mass flow meter. In comparison to the oil-free condition, the heat transfer coefficient generally decreases with oil entrainment regardless of the oil type, which is attributed to the formation of an oil film. A high oil concentration normally corresponds to a significant deterioration in the heat transfer performance.

It can be seen from Fig. 6 that for PAG, the heat transfer coefficient decreases with an increase in the oil concentration at both low and high temperatures. This is caused by the poor miscibility of PAG oil and $CO_2$. For PVE, the increasing oil concentration does not lead to a remarkable decrease in the heat transfer coefficient at low temperatures, because the oil film is not present at low temperature. As the temperature approaches the pseudocritical temperature, the formation of an oil film leads to a decrease in the heat transfer coefficient, and this decrease becomes more significant with an increase in the oil concentration. For ECP, as shown in Fig. 8, the decrease in the heat transfer coefficient with the oil concentration at low temperatures is not significant, whereas at high temperatures, the decrease in the heat transfer coefficient is proportional to the oil concentration.

Figure 9 shows the deterioration factors for the three oils, the values of which range from 0.1 to 0.62 according to the inlet temperature, mass flux, pressure, and oil type. PAG has the largest value, which indicates that it has the largest decrease in the heat transfer coefficient. The values for ECP and PVE are similar at low temperatures. From Fig. 9, it can be seen that the deterioration factor increases with temperature until the bulk temperature approaches the pseudocritical temperature. This is due to decreases in both the solubility of $CO_2$ within the oil and the $CO_2$ density. Above the pseudocritical temperature, the deterioration factor begins to decrease with temperature. When the inlet temperature of the bulk $CO_2$ is lower than the pseudocritical temperature, the heat transfer coefficient of the $CO_2$-ECP mixture is almost equal to that of the $CO_2$-PVE mixture, and both are larger than that of the $CO_2$-PAG mixture. The main reason for this is that it is difficult for the oil film to form given the relatively good miscibility of $CO_2$ and oil at this temperature, and therefore, the heat resistance of the oil film is small. However, the situation is slightly different when the inlet temperature of $CO_2$ approaches the pseudocritical temperature; the heat transfer coefficient of the $CO_2$-PVE mixture is the highest while that of the $CO_2$-PAG mixture is the lowest. When the inlet temperature continues to rise above the pseudocritical temperature, the heat transfer coefficient of the $CO_2$-ECP mixture is still lower than that of the $CO_2$-PVE mixture but close to that of the $CO_2$-PAG mixture.

Near the pseudocritical temperature, a drastic deterioration in the heat transfer coefficient caused by the oil can be observed. Table 3 shows the heat transfer coefficient of the mixture at different values of oil concentration, pressure, and mass flux. Oil with good $CO_2$ solubility has a higher heat transfer coefficient. The growth of the oil film with high solubility is retarded, and therefore, the heat resistance of this film is smaller than that of other oils. It is reasonable to conclude that high solubility of the oil can aid in improving the heat transfer performance.

## 5. CONCLUSIONS

1) The flow patterns of the two-phase fluid for the different oils indicate a remarkable difference in the heat transfer performance.
2) For oils with good solubility with $CO_2$ and an inlet temperature for bulk $CO_2$ lower than the pseudocritical temperature, a sharp deterioration in the heat transfer can be prevented owing to

the difficulty in oil-film formation. When the inlet temperature is above the critical temperature, oils with good solubility form a thin oil film, which slows the deterioration during heat transfer.
3) Visualization experiments indicated that PAG easily forms a thick oil film because of the poor miscibility of PAG and $CO_2$. ECP is inferior to PVE, but shows better heat transfer performance than PVG.

**ACKNOWLEDGEMENTS**
The authors express their gratitude to Idemitsu Kosan Company for providing PAG, PVE and ECP oils. The first author received partial financial support by a Grant-in-Aid for Young Scientists from the Japanese Ministry of Education, Culture, Sports, Science and Technology under Grant No. 18860021.

## REFERENCES

Dang, C., Hihara, E., 2004. In tube cooling heat transfer of supercritical carbon dioxide Part 1: Experimental measurement. Int. J. Refrig. 27, 736-747.
Dang, C., Iino, K., Hihara, E., 2007. Effect of lubricating oil on cooling heat transfer of supercritical carbon dioxide. Int. J. Refrig. 30, 724-731.
Dang, C., Iino, K., Hihara, E., 2008. Study on two-phase flow pattern of supercritical carbon dioxide with entrained PAG-type lubricating oil in a gas cooler. Int. J. Refrig. 31, 1265-1272.
Fang, X., Bullard, C.W., Hrnjak, P.S., 2001. Modeling and analysis of gas coolers. ASHRAE Trans. 107 (1), 4-13.
Gao, L., Honda, T., 2002. Experiments on heat transfer characteristics of heat exchanger for $CO_2$ heat pump system. Proc. Asian Conference on Refrigeration and Air Conditioning 2002, JSRAE, Kobe, Japan. 12, p. A2-A4.
Hwang, Y., Lee, J., Radermacher, R., 2007. Oil distribution in a transcritical CO2 air-conditioning system. Appl. Therm. Eng. 27, 2618-2625.
Kaneko, M., Ikeda, H., Tokiai, T., Yoshii, A., Suto, H., 2006. The development of PAG refrigeration lubricants for automotive A/C with CO2. Proc. JSAE Symp., Tokyo, Japan, 142-159.
Kaneko, M., Ikeda, H., Tokiai, T., Nagao, S., Suto, H., Tamano, M., 2008. The development of PAG-PVE copolymer (ECP). Proc. Int. Symp. on New Refrigerants and Environmental Technology 2008, JSRAE, Kobe, Japan, 376-388.
Sawada, K., 2008. Latest development trends of ester-type refrigeration oils. Proc., Int. Symp. on New Refrigerants and Environmental Technology 2008, JSRAE, Kobe, Japan, 419-432.
Tanaka, H., Nishiwaki, N., Hirata, M., 1967. Turbulent heat transfer to supercritical carbon dioxide. Proc. JSME Semi-International Symp., Tokyo, 127-134.
Yun, R., Hwang, Y., Radermacher, R., Gas cooling heat transfer and pressure drop characteristics of CO2/oil mixture in microchannel. Proc. 7th IIR-Gustav Lorentzen Conference on Natural Working Fluids at Trondheim, Norway, 503-505.
Zingerli A., Groll E.A., 2000. Influence of refrigeration oil on the heat transfer and pressure drop of supercritical CO2 during in-tube cooling. Proc. 4th IIR-Gustav Lorentzen Conference on Natural Working Fluids at Purdue, 269-278.

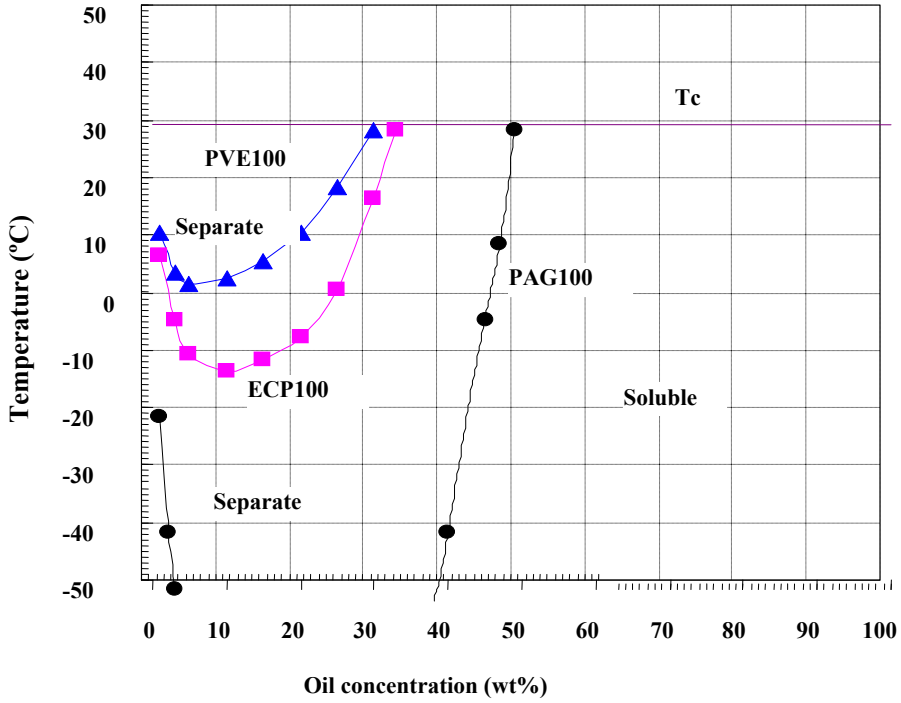


Figure 1: Two-phase separation temperature

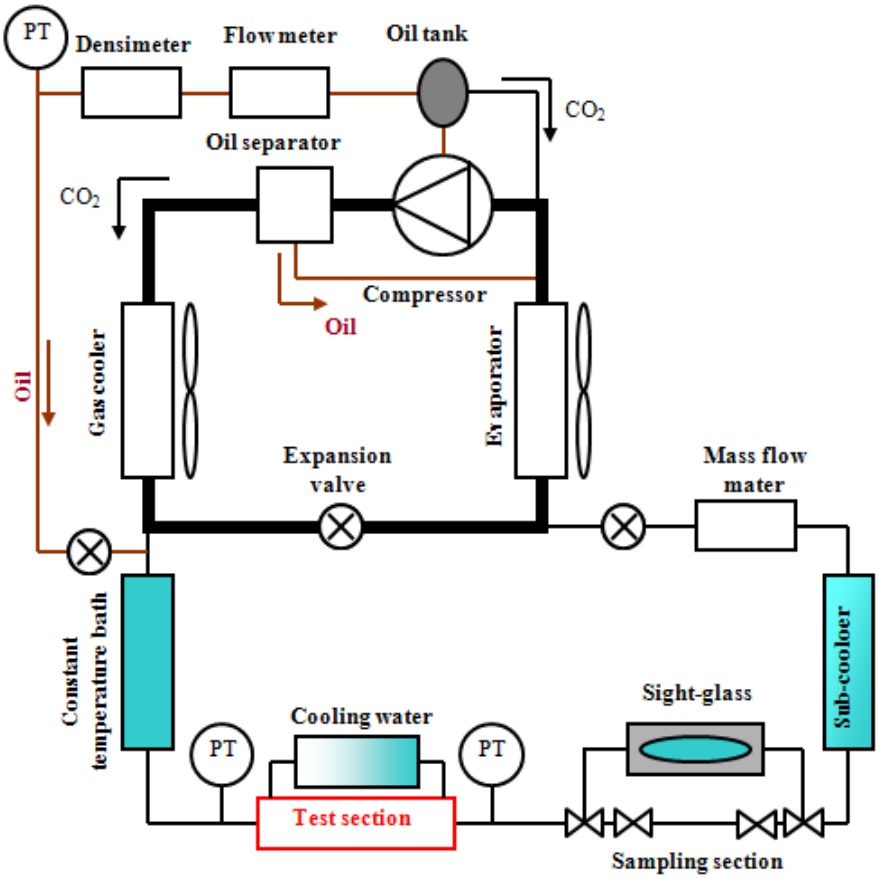


Figure 2: Schematic diagram of experimental apparatus

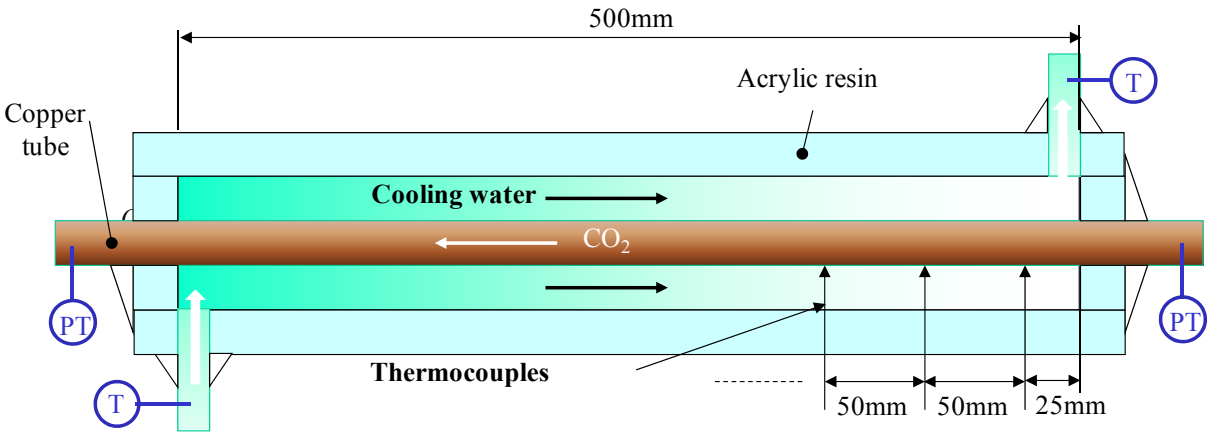


Figure 3: Heat transfer test section

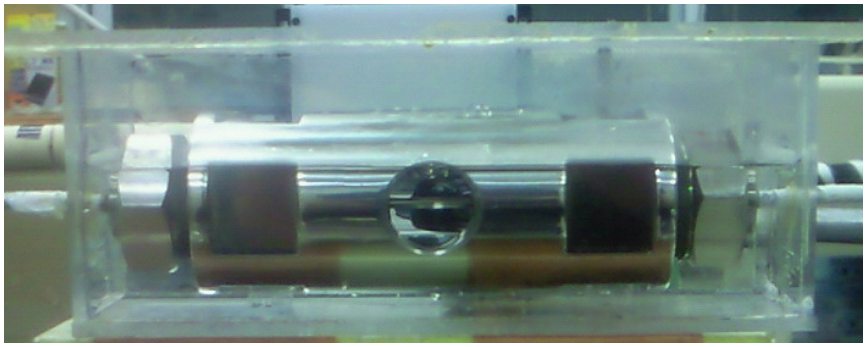

Figure 4: Sight glass

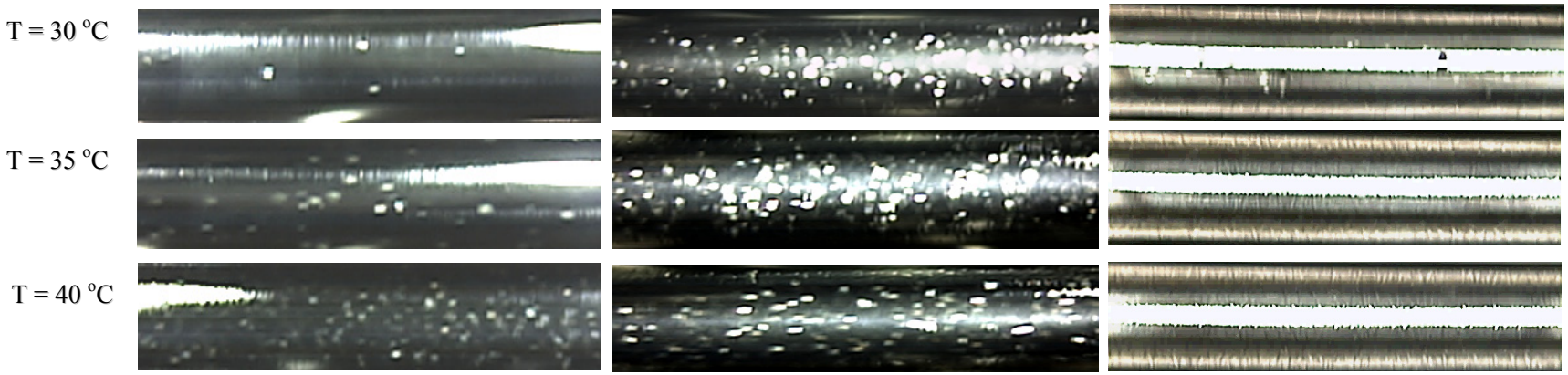


Figure 5: Flow visualization of $CO_2$ with entrained oil; $P$ = 8 MPa, $G$ = 800 kg $m^{-2}s^{-1}$, $x$ = 1 wt%

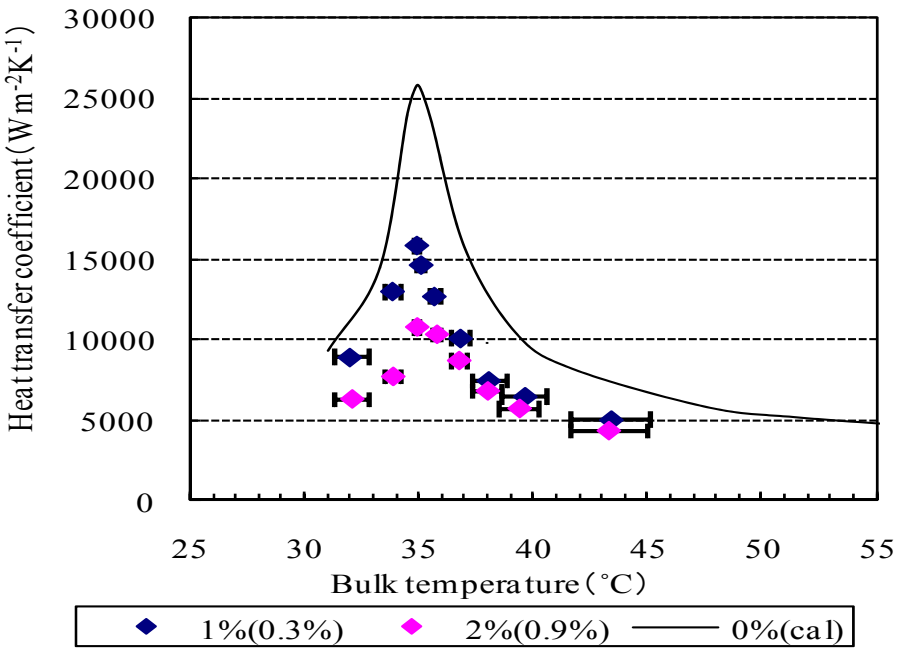


(a) $G$ = 1200 kg m$^{-2}$s$^{-1}$, $P$ = 8 MPa

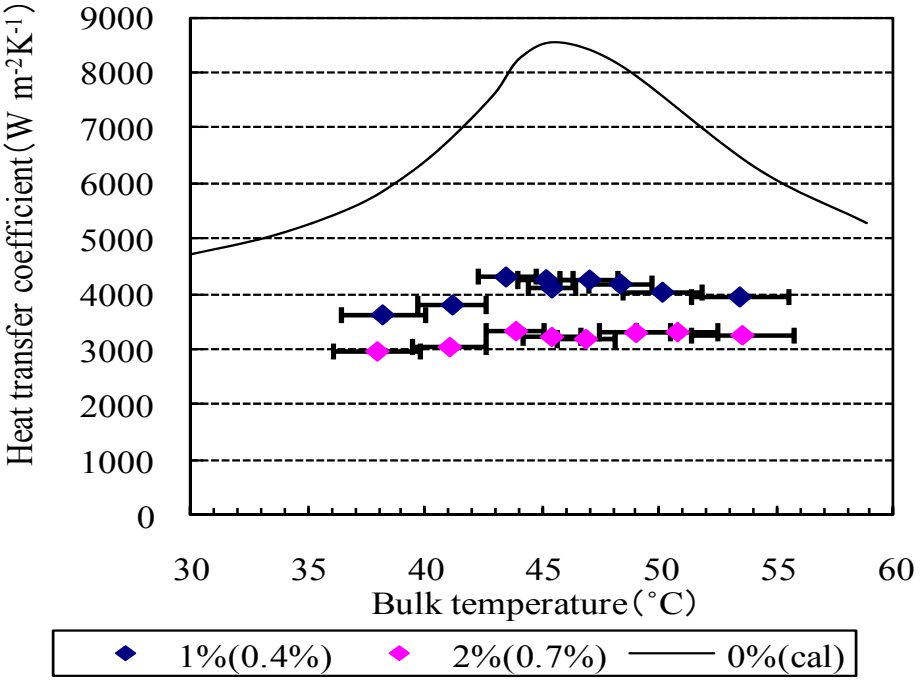


(b) $G$ = 800 kg m$^{-2}$s$^{-1}$, $P$ = 10 MPa

Figure 6: Heat transfer coefficient of $CO_2$-PAG mixture

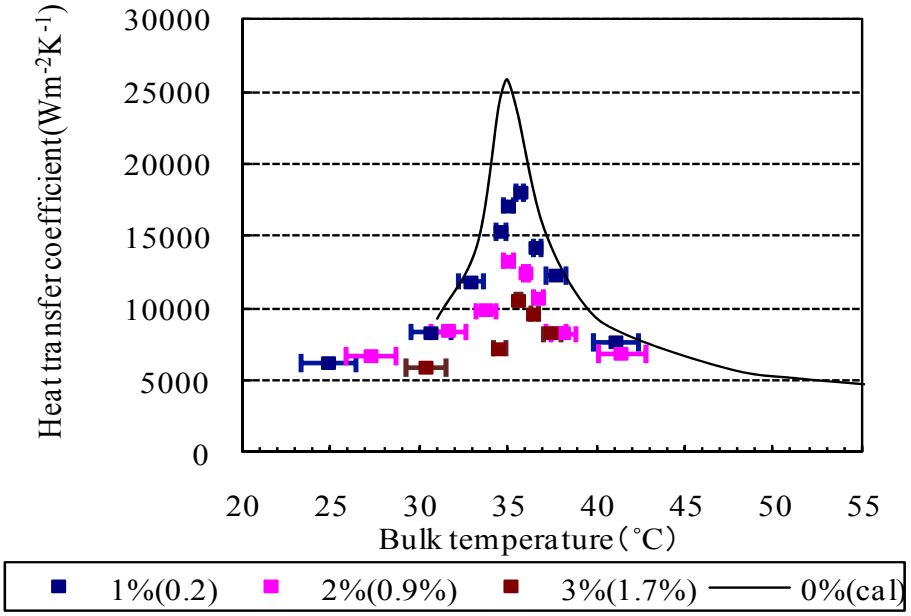


(a) $G$ = 1200 kg m$^{-2}$s$^{-1}$, $P$ = 8 MPa

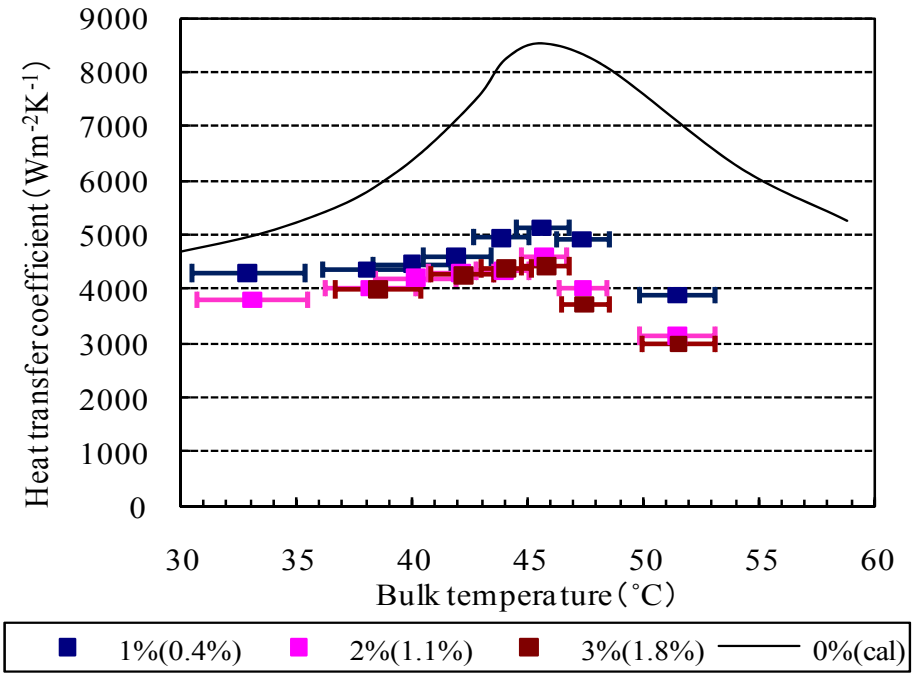


(b) $G$ = 800 kg m$^{-2}$s$^{-1}$, $P$ = 10 MPa

Figure 7: Heat transfer coefficient of $CO_2$-PVE mixture

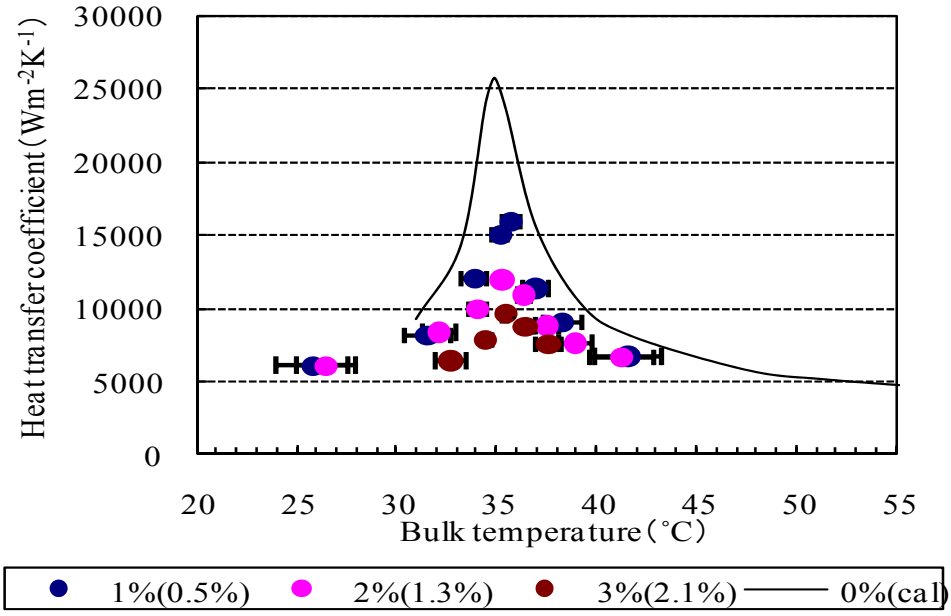


(a) $G$ = 1200 kg m$^{-2}$s$^{-1}$, $P$ = 8 MPa

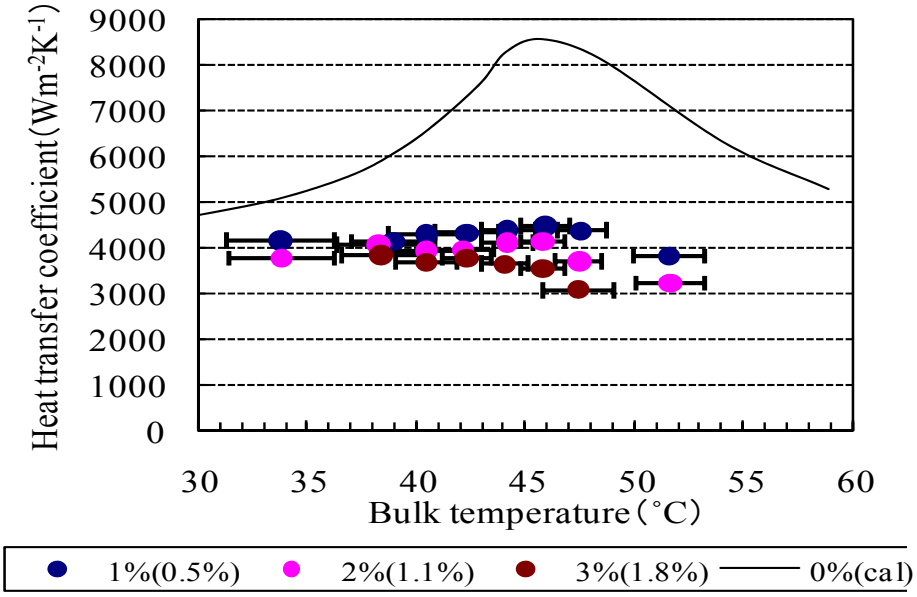


(b) $G$ = 800 kg m$^{-2}$s$^{-1}$, $P$ = 10 MPa

Figure 8: Heat transfer coefficient of $CO_2$-ECP mixture

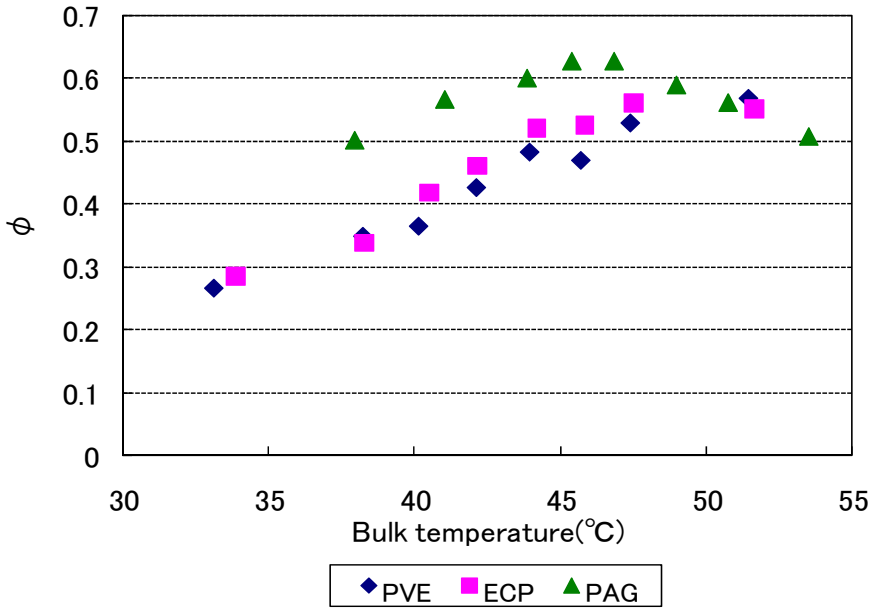


(a) $G$ = 800 kg m$^{-2}$s$^{-1}$, P = 10 MPa, $x$ = 2%

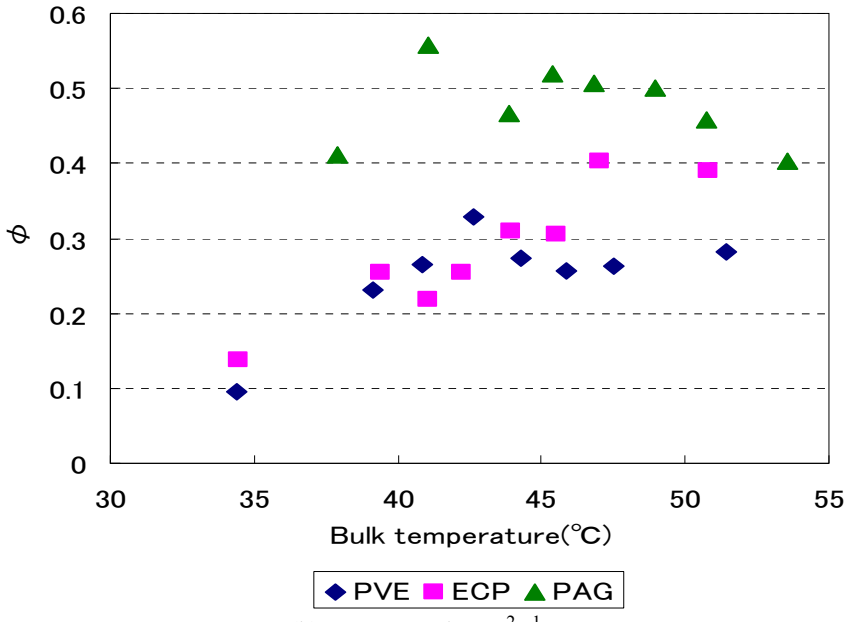


(b) $G$ = 1200 kg m$^{-2}$s$^{-1}$, P = 10 MPa, $x$ = 2%

Figure 9: Deterioration factor of heat transfer coefficient of $CO_2$ for three oils

Table 1: Lubricating oil properties

| Oil type | PAG 100 | PVE 100 | ECP 100 |
|---|---|---|---|
| Molecular structure | 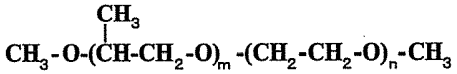 | 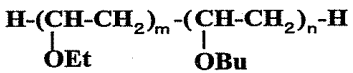 | 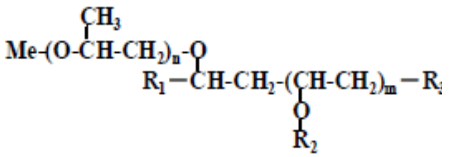 |
| Viscosity at 40 °C | 106.5 $mm^2 s^{-1}$ | 99.2 $mm^2 s^{-1}$ | 100.5 $mm^2 s^{-1}$ |
| Viscosity at 100 °C | 20.47 $mm^2 s^{-1}$ | 10.5 $mm^2 s^{-1}$ | 12.63 $mm^2 s^{-1}$ |
| Viscosity index | 218 | 86 | 120 |
| Thermal conductivity at 20 °C * | 0.156 W $m^{-1} K^{-1}$ | 0.159 W $m^{-1} K^{-1}$ | 0.158 W $m^{-1} K^{-1}$ |
| Thermal conductivity at 80 °C * | 0.145 W $m^{-1} K^{-1}$ | 0.149 W $m^{-1} K^{-1}$ | 0.148 W $m^{-1} K^{-1}$ |

* Provided by Mr. M. Kaneko of Idemitsu Kosan Company through a private communication.

Table 2: Experimental parameters

| | |
|---|---|
| Oil type | PAG, PVE, ECP |
| Tube I.D. (mm) | 2 |
| Pressure (MPa) | 8–10 |
| Mass flux (kg $m^{-2}s^{-1}$) | 800, 1200 |
| Heat flux (kW $m^{-2}$) | 12 |
| Oil concentration (wt%) | 0.5–5 |

Table 3: Comparison of peak value of heat transfer coefficient of $CO_2$-oil mixtures under different conditions

| | $G$ = 800 kg $m^{-2}s^{-1}$, $P$ = 8 MPa, $x$ = 1% | $G$ = 1200 kg $m^{-2}s^{-1}$, $P$ = 8 MPa, $x$ = 2% | $G$ = 800 kg $m^{-2}s^{-1}$, $P$ = 10 MPa, $x$ = 1% | $G$ = 1200 kg $m^{-2}s^{-1}$, $P$ = 10 MPa, $x$ = 2% |
|---|---|---|---|---|
| $CO_2$ + PAG oil | 9645 (W $m^{-2}K^{-1}$) | 10739 (W $m^{-2}K^{-1}$) | 4302 (W $m^{-2}K^{-1}$) | 5682 (W $m^{-2}K^{-1}$) |
| $CO_2$ + ECP oil | 10674 (W $m^{-2}K^{-1}$) | 11944 (W $m^{-2}K^{-1}$) | 4469 (W $m^{-2}K^{-1}$) | 8129 (W $m^{-2}K^{-1}$) |
| $CO_2$ + PVE oil | 12152 (W $m^{-2}K^{-1}$) | 13287 (W $m^{-2}K^{-1}$) | 5138 (W $m^{-2}K^{-1}$) | 8703 (W $m^{-2}K^{-1}$) |